A Compressible Near-Wall Turbulence Model for Boundary Layer Calculations

R. M. C. So, H. S. Zhang and Y. G. Lai*
Mechanical and Aerospace Engineering
Arizona State University
Tempe, AZ 85287-6106, USA

Abstract

A compressible near-wall two-equation model is derived by relaxing the assumption of dynamical field similarity between compressible and incompressible flows. This requires justifications for extending the incompressible models to compressible flows and the formulation of the turbulent kinetic energy equation in a form similar to its incompressible counterpart. As a result, the compressible dissipation function has to be split into a solenoidal part, which is not sensitive to changes of compressibility indicators, and a dilatational part, which is directly affected by these changes. This approach isolates terms with explicit dependence on compressibility so that they can be modeled accordingly. An equation that governs the transport of the solenoidal dissipation rate with additional terms that are explicitly dependent on compressibility effects is derived similarly. A model with an explicit dependence on the turbulent Mach number is proposed for the dilatational dissipation rate. Thus formulated, all near-wall incompressible flow models could be expressed in terms of the solenoidal dissipation rate and straight-forwardly extended to compressible flows. Therefore, the incompressible equations are recovered correctly in the limit of constant density. The two-equation model and the assumption of constant turbulent Prandtl number are used to calculate compressible boundary layers on a flat plate with different wall thermal boundary conditions and free-stream Mach numbers. The calculated results, including the near-wall distributions of turbulence statistics and their limiting behavior, are in good agreement with measurements. In particular, the near-wall asymptotic properties are found to be consistent with incompressible behavior; thus suggesting that turbulent flows in the viscous sublayer are not much affected by compressibility effects.

1. Introduction

Density variation in a turbulent flow can come from different sources. Some of these are: (i) isothermal mixing of gases of different density, (ii) strong temperature gradient in a homogeneous fluid, (iii) reactive flows and (iv) compressibility effects in high speed flows. Each of these sources gives rise to specific aspects that require modeling if the governing equations are to be solved. This study makes an attempt to address the last source; that is, the modeling of high speed compressible turbulent flows.

Most studies on compressible turbulent flow modeling [1-9] invoke the Morkovin postulate [10] to justify the direct extension of the incompressible models to compressible flows. The postulate was formulated based on early experiments on compressible boundary layers along adiabatic walls and compressible wakes, and essentially suggested that the dynamical field in a compressible flow behaves like an incompressible one. This postulate was used by numerous researchers to assure that compressibility effects can be accounted for directly by the variable mean density in the governing equations alone. In other words, the influences of fluctuating density on turbulence mixing are essentially assumed to be negligible. The validity and extent of Morkovin's postulate were reviewed by Bradshaw [2] and he noted that the postulate is appropriate for flows where density fluctuations are moderate. Therefore, the postulate is not valid for hypersonic boundary layers, where the Mach number is five or greater, and for flows with strong pressure gradient effects, such as shock-turbulent-boundary-layer interactions. The latter point was confirmed by the studies of Wilcox and Alber [1] and Bradshaw [11] and led to proposals to have the effects of pressure-dilatation correlation modeled in the governing equations [12]. A more recent study where density fluctuations are also considered has been given by Speziale and Sarkar [13]. Besides these modifications, all turbulent compressible flow modeling rely on incompressible models.

Two sources of difficulties arise when incompressible turbulence models are extended to compressible flows. One is due to compressibility itself and another is associated with the turbulence phenomena. In compressible flows, the governing equations are coupled and temperature cannot be considered as a passive scalar. As a result, all other thermodynamic variables adopt new roles. Therefore, mathematically, compressible flows cannot be considered as straightforward extension of incompressible flows. Furthermore, pressure is only a force term in incompressible flows and all disturbances propagate at infinite speed. On the other hand, pressure also supports finite velocity propagation of disturbances in compressible flows. Other complications come from the variable mean density, which contributes to increased non-linearity of the governing equations, and the fluctuating density, which causes the closure problem to become more difficult.

The second source of difficulties has to do with turbulence mixing. Here, even for incompressible flows, many problems remain to be resolved [14-17], especially when the flow is unsteady and/or three-dimensional [18]. However, among the many problems associated with turbulence modeling, one stands out as most fundamental and urgently needs attention. This is the treatment of the near-wall flow [17]. Conventional approach is to invoke the wall function assumptions; thus implying that near-wall turbulence is in local equilibrium. Even for simple wall shear flows, the assumption is not quite valid because near-wall turbulence is not in local equilibrium. Consequently, a low-Reynolds-number treatment is necessary in order to obtain results that agree with measurements in the near-wall region [17, 19-21]. The need for near-wall treatment of flows with heat and mass transfer has also been pointed out [22-25]. This problem is expected to be more acute in compressible flow modeling [13] where the non-linearity of the governing equations are further compounded by the variable mean density.

The present objective is to model near-wall compressible turbulent flows where the coupling between velocity and temperature cannot be ignored. As a first attempt, only the modeling of the turbulent kinetic energy and its dissipation-rate equations is considered. With the assumption of gradient transport, the two-equation model could be used to effect closure of the mean flow equations. Since the transport equations for the heat fluxes and the temperature dissipation rate are not modeled and solved, a constant turbulent Prandtl number is invoked to relate the heat fluxes to the momentum fluxes. In view of this assumption, the present approach only addresses the issue of compressibility effects on turbulent mixing and not on heat transfer and its interaction with turbulence. An attempt

* Present address: CFD Research Corporation, 3325 Triana Blvd., Huntsville, AL 35805

on this latter problem will be made after the present model has been validated.

2. Proposed Modeling Approach

With the availability of near-wall models for temperature variance and its dissipation rate [24], heat fluxes [25], Reynolds-stresses [26] and the dissipation rate of the turbulent kinetic energy [27], the time is now ripe for their extension to compressible flows. In order to consider the effects of variable mean density and its fluctuation on turbulence mixing, it is necessary to analyse the exact equations and propose appropriate models to effect closure. Two approaches are available. One is to propose totally new models for the terms in the compressible equations, while another is to attempt to extend the incompressible models to compressible flows in a credible way. Both approaches involve assumptions that could or could not be verified experimentally. Since the present knowledge of incompressible flow modeling is quite mature, as a first attempt, it is expedient to extend these models to compressible flows. This can be accomplished by recasting the compressible equations in forms similar to their incompressible counterparts so that terms with explicit dependence on compressibility effects can be isolated separately, and the incompressible limit can be recovered in a straight forward and correct manner.

Since the turbulent kinetic energy equation or k-equation is obtained by contracting the Reynolds-stress equations, this means that the recasting of the Reynolds-stress equations should be attempted first. In other words, the viscous diffusion and dissipation terms in the Reynolds-stress equations have to be similarly defined as their incompressible counterparts. This suggests splitting the viscous dissipation function into a solenoidal part, which is not sensitive to changes of compressibility indicators, and a dilatational part, which is directly affected by these changes[28]. When the Reynolds-stress equations are written in this form, three additional terms that depend explicitly on compressibility effects are present. The k-equation is then obtained by contracting the Reynolds-stress equations and its incompressible counterpart is recovered correctly when density becomes constant and the additional terms vanish identically. An equation that governs the transport of the solenoidal dissipation rate (ε) of the turbulent kinetic energy (k) is derived and modeled along the line suggested above. Again, additional terms that depend explicitly on compressibility effects appear in the equation. This equation also reduces correctly to its modeled incompressible counterpart because the additional terms vanish for constant density flows. All models proposed for the k and ε equations are expressed in terms of this solenoidal dissipation rate. A model with explicit dependence on the turbulent Mach number proposed by Sarkar et al. [28] for the dilatational dissipation is adopted. Thus formulated, the two-equation model is valid for compressible flows and approaches its incompressible limit in a straight forward and correct manner.

The systematic approach described above, if proven successful, could be used to extend incompressible near-wall models for heat-fluxes, temperature variance and its dissipation rate to compressible flows. A set of equations governing the transport of incompressible heat fluxes has been proposed and validated against simple flows with heat transfer [25], while a similar set of equations for the temperature variance and its dissipation rate [24] has also been validated against boundary-layer flows. This means that near-wall heat transfer models could also be extended to compressible flows using the approach proposed above. However, before this extension is undertaken, the asymptotic consistency of these models has to be verified. Until such time, the assumption of a constant turbulent Prandtl number for near-wall compressible flow is inevitable.

In the following, the compressible equations are first derived, then the near-wall modeling of the k and ε equations are discussed. In section 6, the two-equation model is used to calculate compressible boundary layers on a flat plate assuming a constant turbulent Prandtl number. Comparisons with measurements [9, 29-31] and other calculations, such as those obtained using the k-ω model of Wilcox [8], are carried out to assess the importance of density fluctuations on the calculated results and, hence, the validity and extent of Morkovin's hypothesis.

3. Mean Flow Equations

The compressible mean flow equations are obtained by applying Favre averaging to the instantaneous Navier-Stokes equations which for Newtonian fluids can be written as:

$$\frac{\partial \rho}{\partial t} + \frac{\partial}{\partial x_i}(\rho u_i) = 0 \quad , \tag{1}$$

$$\frac{\partial(\rho u_i)}{\partial t} + \frac{\partial}{\partial x_j}(\rho u_i u_j) = -\frac{\partial p}{\partial x_i} + \frac{\partial \tau_{ij}}{\partial x_j} \quad , \tag{2}$$

$$\frac{\partial(\rho C_p T)}{\partial t} + \frac{\partial}{\partial x_i}(\rho C_p T u_i) = \frac{\partial p}{\partial t} + u_i \frac{\partial p}{\partial x_i} + \frac{\partial}{\partial x}\left(\kappa \frac{\partial T}{\partial x_i}\right) + \tau_{ij}\frac{\partial u_i}{\partial x_j} \quad , \tag{3}$$

$$\text{where } \tau_{ij} = \mu\left(\frac{\partial u_i}{\partial x_j} + \frac{\partial u_j}{\partial x_i}\right) - \frac{2}{3}\mu \frac{\partial u_k}{\partial x_k}\delta_{ij} \quad , \tag{4}$$

u_i is the i^{th} component of the velocity vector, x_i is the i^{th} component of the coordinates and p, T, ρ, μ, κ, C_p are pressure, temperature, density, viscosity, thermal conductivity and specific heat at constant pressure, respectively. Favre decomposition is applied to all variables except p and ρ where conventional Reynolds decomposition is assumed. In other words

$$u_i = \langle U_i \rangle + u_i'' \quad , \tag{5}$$

$$T = \langle \Theta \rangle + \theta'' \quad , \tag{6}$$

$$p = \overline{P} + p' \quad , \tag{7}$$

$$\rho = \overline{\rho} + \rho' \quad , \tag{8}$$

where u_i'' and θ'' are the Favre fluctuations and p' and ρ' are the Reynolds fluctuations. If $< >$ is used to denote Favre-averaged quantities and the overbar the Reynolds-averaged quantities, then the mean equations for compressible flows can be obtained as follows. The above decompositions (5)-(8) are substituted into (1)-(4) and the resultant equations are averaged over time. If the turbulent flow is further assumed to be stationary and the mean momentum equation and the Reynolds-stress and turbulent kinetic energy, $k = \frac{1}{2}\langle u_i u_i \rangle$, equations to be derived later are used to simplify the thermal energy equation, the turbulent mean flow equations become

$$\frac{\partial}{\partial x_i}\left(\overline{\rho}\langle U_i \rangle\right) = 0 \quad , \tag{9}$$

$$\frac{\partial}{\partial x_j}\left(\overline{\rho}\langle U_i \rangle\langle U_j \rangle\right) = -\frac{\partial \overline{P}}{\partial x_i} + \frac{\partial \langle \tau_{ij} \rangle}{\partial x_j} - \frac{\partial}{\partial x_j}\left(\overline{\rho}\langle u_i'' \rangle\langle u_j'' \rangle\right) + \frac{\partial \overline{\tau_{ij}''}}{\partial x_j} \quad , \tag{10}$$

$$\frac{\partial}{\partial x_i}\left(\overline{\rho}\langle U_i\rangle\left[\overline{C}_p\langle\Theta\rangle + \tfrac{1}{2}\langle U_k\rangle\langle U_k\rangle + k\right]\right)$$

$$= \frac{\partial}{\partial x_i}\left(\overline{\kappa}\frac{\partial\langle\Theta\rangle}{\partial x_i}\right) + \frac{\partial}{\partial x_j}\left(\langle\tau_{ij}\rangle\langle U_i\rangle\right) - \frac{\partial}{\partial x_i}\left(\overline{\rho}\,\overline{C}_p\langle\theta'' u_i''\rangle\right)$$

$$- \frac{\partial}{\partial x_i}\left(\overline{\rho}\langle u_i'' u_j''\rangle\langle U_j\rangle\right) + \underline{\frac{\partial}{\partial x_i}\left(\overline{\tau_{ij}''}\langle U_j\rangle\right)} - \underline{\frac{\partial}{\partial x_i}\left(\overline{\rho}\langle k\, u_i''\rangle\right)}$$

$$+ \underline{\frac{\partial}{\partial x_i}\left(\overline{u_j''\tau_{ij}''}\right)} + \underline{\frac{\partial}{\partial x_i}\left(\overline{u_j''}\langle\tau_{ij}\rangle\right)} + \underline{\frac{\partial}{\partial x_i}\left(\overline{\kappa}\,\overline{\frac{\partial\theta''}{\partial x_i}}\right)} \quad . \tag{11}$$

In these equations, $\mu = \overline{\mu}$, $\kappa = \overline{\kappa}$ and $C_p = \overline{C}_p$ have been substituted and the mean and fluctuating stresses are given by

$$\langle\tau_{ij}\rangle = \overline{\mu}\left(\frac{\partial\langle U_i\rangle}{\partial x_j} + \frac{\partial\langle U_j\rangle}{\partial x_i}\right) - \frac{2}{3}\overline{\mu}\,\delta_{ij}\frac{\partial\langle U_k\rangle}{\partial x_k} \quad ,$$

$$\overline{\tau_{ij}''} = \overline{\mu}\left(\overline{\frac{\partial u_i''}{\partial x_j}} + \overline{\frac{\partial u_j''}{\partial x_i}}\right) - \frac{2}{3}\overline{\mu}\,\delta_{ij}\overline{\frac{\partial u_k''}{\partial x_k}} \quad .$$

The quantity, $\overline{C}_p\langle\Theta\rangle + \frac{1}{2}\langle U_k\rangle\langle U_k\rangle + k$, is the mean total enthalpy $\langle H\rangle$. Thus written, (9)-(11) reduce to their incompressible counterparts exactly when density becomes constant.

An order-of-magnitude analysis is carried out on (9) - (11). The result shows that the underlined terms are of smaller order and, as a first approximation, could be neglected compared to the terms retained. Thus formulated, the compressible equations are identical to the incompressible equations and the additional unknowns are the turbulent momentum and heat fluxes, just as in the incompressible case. The present approach proposes to close these equations assuming gradient transport. As a first attempt, a near-wall two-equation k-ε model is used to determine the turbulent viscosity and a constant turbulent Prandtl number is invoked to relate turbulent momentum and heat fluxes. Therefore, the present model cannot fully account for the effects of density fluctuation on turbulent heat transfer.

4. Modeling of the Turbulent Kinetic Energy Equation

The Favre-averaged transport equation for the Reynolds stresses $\overline{\rho}\langle u_i'' u_j''\rangle$ could be similarly derived as in the incompressible case [16]. That is, the ith fluctuating velocity equation is obtained by subtracting the mean momentum equation from the instantaneous equation. Repeat the same procedure to obtain the jth fluctuating velocity equation. The ith fluctuating velocity equation is then multiplied by the jth fluctuation velocity and vice versa and the two equations are added together and averaged over time. Omitting all the algebra, the final exact equation is:

$$\frac{\partial}{\partial t}\left[\overline{\rho}\langle u_i'' u_j''\rangle\right] + \frac{\partial}{\partial x_k}\left[\overline{\rho}\langle U_k\rangle\langle u_i'' u_j''\rangle\right] = -\frac{\partial}{\partial x_k}\left[\overline{\rho}\langle u_i'' u_j'' u_k''\rangle\right]$$
$$+ \frac{\partial}{\partial x_k}\left[\overline{u_i''\tau_{jk}''} + \overline{u_j''\tau_{ik}''}\right] - \left[\overline{\tau_{ik}''\frac{\partial u_j''}{\partial x_k}} + \overline{\tau_{jk}''\frac{\partial u_i''}{\partial x_k}}\right]$$
$$- \left[\overline{u_i''\frac{\partial p'}{\partial x_j}} + \overline{u_j''\frac{\partial p'}{\partial x_j}}\right] - \left[\overline{\rho}\langle u_i'' u_k''\rangle\frac{\partial\langle U_j\rangle}{\partial x_k} + \overline{\rho}\langle u_j'' u_k''\rangle\frac{\partial\langle U_i\rangle}{\partial x_k}\right] \tag{12}$$
$$- \left[\overline{u_i''}\frac{\partial\overline{P}}{\partial x_j} + \overline{u_j''}\frac{\partial\overline{P}}{\partial x_i}\right] + \left[\overline{u_i''}\frac{\partial\langle\tau_{jk}\rangle}{\partial x_k} + \overline{u_j''}\frac{\partial\langle\tau_{ik}\rangle}{\partial x_k}\right] \quad .$$

Symbolically, the above equation can be written as

$$C_{ij} = D_{ij}^T + D^{*\nu}_{ij} - \overline{\rho}\,\varepsilon^*_{ij} + \Phi_{ij} + P_{ij} + G_{ij} + T_{ij} \quad . \tag{13}$$

With the exception of G_{ij} and T_{ij}, (13) is similar to its incompressible counterpart [26]. For an incompressible flow, $u_i \equiv 0$, and $G_{ij} = T_{ij} = 0$. Even under this condition, (13) fails to reduce properly to the incompressible equation given in Ref. 26. The reason lies in the grouping of the terms $\left(D^{*\nu}_{ij} - \overline{\rho}\varepsilon^*_{ij} + \Phi_{ij}\right)$. In order to achieve this incompressible limit correctly, a re-arranging of the terms in $\left(D^{*\nu}_{ij} - \overline{\rho}\varepsilon^*_{ij} + \Phi_{ij}\right)$ is necessary. If viscous diffusion and dissipation in compressible flows are again defined similarly to their incompressible counterparts, or

$$D^{\nu}_{ij} = \frac{\partial}{\partial x_k}\left(\overline{\mu}\,\overline{\frac{\partial u_i'' u_j''}{\partial x_k}}\right) , \tag{14}$$

$$\varepsilon_{ij} = 2\overline{\nu}\,\overline{\frac{\partial u_i''}{\partial x_k}\frac{\partial u_j''}{\partial x_k}} , \tag{15}$$

then the terms $\left(D^{*\nu}_{ij} - \overline{\rho}\varepsilon^*_{ij} + \Phi_{ij}\right)$ can be re-arranged to give

$$D^{*\nu}_{ij} - \overline{\rho}\,\varepsilon^*_{ij} + \Phi_{ij} = D^{\nu}_{ij} - \overline{\rho}\,\varepsilon_{ij} - \overline{\rho}\,\varepsilon^c_{ij} + \Phi^*_{ij} \tag{16}$$

where $\varepsilon^c_{ij} = \frac{\overline{\nu}}{3}\left(\overline{\frac{\partial u_i''}{\partial x_j}\frac{\partial u_k''}{\partial x_k}} + \overline{\frac{\partial u_j''}{\partial x_i}\frac{\partial u_k''}{\partial x_k}}\right)$, (17a)

$$\Phi^*_{ij} = -\left[\overline{u_i''\frac{\partial p'}{\partial x_j}} + \overline{u_j''\frac{\partial p'}{\partial x_i}}\right] + \frac{\overline{\mu}}{3}\left[\frac{\partial}{\partial x_j}\left(\overline{u_i''\frac{\partial u_k''}{\partial x_k}}\right)\right.$$
$$\left. + \frac{\partial}{\partial x_i}\left(\overline{u_j''\frac{\partial u_k''}{\partial x_k}}\right)\right] + \frac{\partial\overline{\mu}}{\partial x_k}\left(\overline{u_i''\frac{\partial u_k''}{\partial x_j}} + \overline{u_j''\frac{\partial u_k''}{\partial x_i}}\right)$$
$$- \frac{2}{3}\left[\frac{\partial\overline{\mu}}{\partial x_j}\overline{u_i''\frac{\partial u_k''}{\partial x_k}} + \frac{\partial\overline{\mu}}{\partial x_i}\overline{u_j''\frac{\partial u_k''}{\partial x_k}}\right] . \tag{17b}$$

Note that (16) reduces to its incompressible counterpart exactly when constant fluid properties are assumed. For compressible flows, an extra term $\overline{\rho}\,\varepsilon^c_{ij}$ appears in (16). In addition, three additional terms are found in Φ^*_{ij}. The term $\overline{\rho}\,\varepsilon^c_{ij}$ is a dilatational term and could be interpreted as compressible or dilatational dissipation. This term is only important for compressible flows.

It should be pointed out that Φ^*_{ij} is given by (17b) and, as a result of this particular partitioning, there are several extra terms resulted from compressibility and variable viscosity. However, at high Reynolds number, dimensional arguments reveal that these extra contributions are not important. If pressure diffusion is further neglected, then D^{ν}_{ij}, $\overline{\rho}\,\varepsilon_{ij}$ and Φ_{ij} would assume the same form as their incompressible counterparts. Therefore, the high-Reynolds-number incompressible models proposed for these terms [16, 32] could be straight-forwardly extended to compressible flows. However, a model for the compressible dissipation term $\overline{\rho}\,\varepsilon^c_{ij}$ is

required to complete closure. For high-Reynolds-number flows, this compressible dissipation could be assumed to be isotropic. As a result, the following model is proposed:

$$\varepsilon_{ij}^c = \frac{2}{3}\delta_{ij}\varepsilon^c \qquad (18)$$

where $\varepsilon^c = \overline{\nu}\overline{\left(\frac{\partial u_k''}{\partial x_k}\right)^2}$.

The modeling of ε^c has been attempted by Sarkar et al. [28]. They are the first to realize that the contribution of the dilatational dissipation term is important for supersonic shear flows. A simple algebraic model, which is based on an asymptotic analysis and a direct numerical simulation of the simplified governing equations, has been proposed for ε^c. Their proposal could be modified to become

$$\varepsilon^c = \alpha_1 M_t^2 \varepsilon \quad , \qquad (19)$$

where α_1 is a model constant, $M_t^2 = 2k/\overline{c}^2$, $\overline{\rho}\varepsilon = \overline{\mu}\overline{\left(\frac{\partial u_i''}{\partial x_k}\right)^2}$ is the dissipation of k and $\overline{c}$ is the local mean speed of sound. Therefore, M_t is the local turbulent Mach number. It should be pointed out that Sarkar et al.'s [28] definition of ε^c is four times larger than the definition given in (19) as a result of a different splitting of the terms in (16). Consequently, α_1 should take on a value equal to 1/4 of that suggested in Ref. 28. Based on an analysis of decay of compressible isotropic turbulence, Sarkar et al. [28] suggested a value of one for their constant. In other words, $\alpha_1 = 0.25$. If α_1 is evaluated based on compressible shear flows, its value would be 0.15. The present study adopts $\alpha_1 = 0.15$ for the analyses of boundary-layer flows.

The k-equation is obtained by contracting (12) and making use of (16) and (18) to simplify the resulting equation which can be written as:

$$\frac{D(\overline{\rho}k)}{Dt} = D_k^v + D_k^T + \frac{1}{2}P_{ii} + \frac{1}{2}\Phi_{ii}^* - \frac{1}{2}\overline{\rho}\varepsilon_{ii} - \frac{1}{2}\overline{\rho}\varepsilon_{ii}^c$$

$$+ \frac{1}{2}G_{ii} + \frac{1}{2}T_{ii} \quad . \qquad (20)$$

It can be seen that the terms, D_k^T, Φ_{ii}^* and $\overline{\rho}\varepsilon_{ii}$, and the coefficient, u_i, appearing in G_{ii} and T_{ii} require modeling. Furthermore, when ρ is assumed to be constant and $u_i = 0$, the last three terms in (20) are identically zero and the incompressible equation is recovered exactly. The modeling of D_k^T, Φ_{ii} and $\overline{\rho}\varepsilon_{ii}$ could be accomplished by drawing parallels with their incompressible counterparts [26, 27]. However, this requires knowledge of their behavior in the near-wall region.

The near-wall behavior of (20) can be analysed by assuming Taylor series expansions about the wall for the fluctuating quantities. This analysis is similar to the incompressible case [26] except that expansions also have to be assumed for ρ' and θ''. The proposed expansions are:

$$\begin{aligned} u'' &= a_1 y + a_2 y^2 + \ldots, \\ v'' &= b_1 y + b_2 y^2 + \ldots, \\ w'' &= c_1 y + c_2 y^2 + \ldots, \\ \theta'' &= d_1 y + d_2 y^2 + \ldots, \\ \rho' &= e_1 y + e_2 y^2 + \ldots. \end{aligned} \qquad (21)$$

It should be cautioned that, although the velocity and temperature expansions are physically correct, the expansion for density is an assumption. As pointed out by Bradshaw [11], the fluctuating temperature and density could not go to zero simultaneously at the wall. Otherwise, it would lead to a zero wall p'. In general, temperature fluctuation is assumed to be zero at the wall, while ρ' is not. Here, the assumption is made that ρ' also goes to zero at the wall, however, its value away from the wall is finite. Since ρ' is taken to be essentially zero over the whole field in Morkovin's hypothesis [10], the present approach could be viewed as a partial relaxation of that assumption. Consequently, the proposed model would not be valid for all free-stream Mach number and wall thermal boundary conditions. Therefore, one of the present objective is to analyse the validity and extent of the proposed two-equation model.

For incompressible flows, $b_1 = 0$ is obtained by imposing the incompressibility condition and becomes a crucial condition in near-wall analysis. This important condition holds the key to the present extension of the near-wall incompressible models to compressible flows. In order to show that b_1 indeed vanishes under these conditions, the continuity equation for ρ' is first derived, or

$$\frac{\partial \rho'}{\partial t} + \frac{\partial}{\partial x_k}\left(\overline{\rho}u_k'' + \rho'\langle U_k\rangle + \rho' u_k''\right) = 0. \qquad (22)$$

Expansions (21) are then substituted into the above equation. If $\langle U_k\rangle = 0$ at the wall is used, it can be easily verified that, under the assumption of (21), $b_1 = 0$ is still a valid condition for compressible flows, irrespective of the thermal boundary condition. Therefore, the assumed ρ' expansion facilitates the modeling of compressible flows, because all terms in (20) have similar forms as their incompressible counterparts except the extra ε_{ii}^c term which needs to be analyzed.

Using definition (18) for ε_{ij}^c, it is easily verified that ε_{ii}^c is of order y^2. The high-Reynolds-number model (19) also has similar behavior near a wall. Therefore, it is proposed to extend (19) to near-wall flow without modification, while the near-wall balance provided by the exact ε_{ii}^c is taken into consideration by combining it with the Φ_{ii} term. As for $\overline{\rho}\varepsilon_{ii}$, it could be modeled by following the arguments presented in Refs. 26 and 27 for incompressible flows. In essence, Refs. 26 and 27 argue that the incompressible ε_{ij} can be set equal to 2ε and the near-wall corrections proposed for ε_{ij} have little or no effects on the behavior of ε_{ii} in the region near a wall. This means that ε_{ii} can be approximated by 2ε in the whole field. In view of this, the model for $\overline{\rho}\varepsilon_{ii}$ can be assumed to be given by $2\overline{\rho}\varepsilon$. Based on this model, equation (15) and expansions (21), it can be easily shown that the leading term of ε in the near-wall region is a constant equal to its wall value ε_w. Again, the behavior is similar to its incompressible counterpart.

Near-wall analysis again shows that turbulent diffusion is a higher order term and its high-Reynolds-number model could be adopted because it does not affect near-wall balance of the k-equation. Consistent with the assumption of gradient transport for two-equation models, the incompressible model for turbulent diffusion of k is extended to compressible flows by writing $D_k^T = \partial((\overline{\mu}_t/\sigma_k)\partial k/\partial x_i)/\partial x_i$, where σ_k is a constant and $\overline{\mu}_t$ is the turbulent viscosity defined by $\overline{\mu}_t = C_\mu f_\mu \overline{\rho} k^2/\varepsilon$. In this definition, C_μ is a model constant while f_μ is a damping function to be defined later. Based on (21), the leading order term of k in the near-wall region is y^2. Since $\varepsilon = \varepsilon_w$ in this region, k^2/ε has to be of order y^4. If the shear stress is defined with respect to $\overline{\mu}_t$, then it can be shown that the leading order term of the shear stress has to be of order y^3 in the near-wall region. Therefore, it follows that $\overline{\nu}_t = \overline{\mu}_t/\overline{\rho}$ is also of order y^3 near a wall and this,

in turn, leads to a similar behavior for the modeled D_k^T term in the near-wall region. This behavior is consistent with the behavior of the exact term D_k^T appearing in (20). In other words, the modeled D_k^T does not affect the near-wall balance of (20).

According to (18), $\varepsilon_{ii}^c = 2\varepsilon^c$. As such, the near-wall behavior of the exact ε_{ii}^c is not properly accounted for by the proposed model. In the above discussion, it is argued that the near-wall behavior of ε_{ii}^c could be modeled together with the term Φ_{ii}. In order to analyse the near-wall behavior of the combined term $(\Phi_{ii}^* + \overline{\rho}\varepsilon_{ii}^c)$, the behavior of G_{ii} and T_{ii} near a wall has to be studied. The appearance of mean pressure in G_{ii} makes the analysis slightly more difficult. However, the difficulty could be circumvented by making use of the mean momentum equation (10). The final analysis shows that the combined $(G_{ii} + T_{ii})$ term has the following near-wall behavior; namely,

$$G_{11} + T_{11} \to O(y^2)\,;\; G_{33} + T_{33} \to O(y^2)\,;$$
$$G_{22} + T_{22} \to O(y^3)\quad . \tag{23}$$

This means that, to the lowest order, the near-wall behavior of $(\Phi_{ii} + \overline{\rho}\varepsilon_{ii}^c)$ is similar to its incompressible counterpart [26]. For incompressible flows, the term, Φ_{ii}, can be written into a pressure diffusion part and a pressure redistribution part. Pressure redistribution is identically zero and since pressure diffusion is relatively small, it is usually neglected. Such is not the case for compressible flows. The term, Φ_{ii}, can again be partition into a pressure diffusion part, which could be neglected, and a term involving pressure-velocity-gradient correlation. This latter term does not vanish because fluid volume changes as a result of density variation. Therefore, an argument could be made to model the term, $(\Phi_{ii}^* + \overline{\rho}\varepsilon_{ii}^c)$, to account for dilatational effects only. In view of this, the following model is proposed, or

$$(\Phi_{ii}^* + \overline{\rho}\varepsilon_{ii}^c) = -\gamma\overline{\rho}\,k\left(\frac{\partial\langle U_i\rangle}{\partial x_i}\right)\quad , \tag{24}$$

where γ is a model constant.

The proposed models still fail to close the k-equation because of the presence of $\overline{u_i''}$ in T_{ii} and G_{ii}. Therefore, it is necessary to shed some light on the modeling of $\overline{u_i''}$, which is identically zero for incompressible flows. Using Favre averaging, it can be shown that $-\overline{\rho' u_i''} = \overline{\rho u_i''}$. In other words, $\overline{u_i''} = -\overline{\rho' u_i''}/\overline{\rho}$. Previous proposals for $-\overline{\rho' u_i''}$ are based on the gradient transport assumption; namely,

$$-\overline{\rho' u_i''} = \frac{\overline{\nu}_t}{\sigma_\rho}\frac{\partial\overline{\rho}}{\partial x_i}\,, \tag{25}$$

where σ_ρ is a model constant. However, a more elaborate way to model the term is to adopt the proposal,

$$\overline{u_i''} = -\frac{\overline{\rho' u_i''}}{\overline{\rho}} = C_\rho\frac{k}{\rho\varepsilon}\langle u_i'' u_j''\rangle\frac{\partial\overline{\rho}}{\partial x_j}\quad , \tag{26}$$

where C_ρ is a model constant. Alternatively, the term can also be modeled by

$$\overline{u_i''} = \beta\frac{\overline{u_i''\theta''}}{\langle\Theta\rangle}\,,\quad \text{with } \beta = -\left(\frac{\partial\overline{\rho}}{\partial\langle\Theta\rangle}\right)_p\frac{\langle\Theta\rangle}{\overline{\rho}}\quad , \tag{27}$$

where β equals to unity for an ideal gas.

The near-wall behavior of the modeled k-equation can now be analysed using expansions (21). It can be easily shown that in the region very near a wall, the modeled k-equation is in balance up to order y. Consequently, it does not need further modifications to achieve a consistent asymptotic behavior near a wall.

5. Modelling of the Dissipation-Rate Equation

The exact transport equation for the solenoidal dissipation rate $(\overline{\rho}\varepsilon)$ can be derived as in the Reynolds-stress equation (12). It has been pointed out that the ε-equation is the most difficult to model even for incompressible flows [13, 16, 17, 26, 27, 32]. The reason being that many of the terms in the exact equation are either not known or could not be measured accurately at present. Consequently, the incompressible ε-equation is modeled in an ad hoc manner to resemble the k-equation in form so that the right hand side of the ε-equation again consists of four terms; namely, viscous diffusion, turbulent diffusion, production and destruction of ε. The equation is further modified for near-wall flows by adding an extra destruction term ξ so that the modeled equation remains balance as a wall is approached. There is a lack of measurements in compressible flows, therefore, a rigorous modeling of the compressible ε-equation is not possible at present. An alternative is to extend the high-Reynolds-number incompressible models to compressible flows and then seek a near-wall correction to the modeled ε-equation along the line suggested in Ref. 27. In view of this, the exact transport equation for the dissipation rate is not in a convenient form to work with. The proposal of Speziale and Sarkar [13] with the dilatational effects explicitly written out will be more appropriate.

Following Speziale and Sarkar [13], the modeled transport equation for ε with near-wall correction is written in the simplified form; namely

$$\frac{D\overline{\rho}\varepsilon}{Dt} = \frac{\partial}{\partial x_i}\left(\overline{\mu}\frac{\partial\varepsilon}{\partial x_i}\right) + D_\varepsilon^t + P_\varepsilon - \Delta_\varepsilon - \frac{4}{3}\overline{\rho}\varepsilon\frac{\partial\langle U_i\rangle}{\partial x_i} + \xi\,, \tag{28}$$

where D_ε^t is the turbulent transport of ε, P_ε is the production of ε due to deviatoric strains, Δ_ε is the destruction of ε and ξ is a near-wall correction for compressible flows. The second last term on the right hand side of (28) is exact and results from the writing of the exact ε-equation into the form of (28). When the dissipation-rate equation is formulated in this form, it is reducible exactly to its incompressible counterpart and, therefore, the terms D_ε^t, P_ε and Δ_ε can be modeled by a variable density extension of their incompressible models. Following the suggestions of Refs. 13 and 27, the models proposed for D_ε^t, P_ε and Δ_ε are:

$$D_\varepsilon^t = \frac{\partial}{\partial x_i}\left(\frac{\overline{\mu_t}\,\partial\varepsilon}{\sigma_\varepsilon\partial x_i}\right), \tag{29a}$$

$$P_\varepsilon = -C_{\varepsilon 1}\overline{\rho}\frac{\varepsilon}{k}\left(u_i'' u_j''\right)\left(\frac{\partial\langle U_i\rangle}{\partial x_j} - \frac{1}{3}\frac{\partial\langle U_k\rangle}{\partial x_k}\delta_{ij}\right), \tag{29b}$$

$$\Delta_\varepsilon = C_{\varepsilon 2}\overline{\rho}\frac{\tilde{\varepsilon}\tilde{\varepsilon}}{k}\,, \tag{29c}$$

where the model constants $C_{\varepsilon 1}$ and $C_{\varepsilon 2}$ are the same as those given in Ref. 27 for incompressible flows and $\tilde{\varepsilon} = \varepsilon - \varepsilon_w$. It should be noted that the mean dilatational effects are accounted for exactly by (29b) for compressible flows and that these models reduce exactly to their incompressible counterparts when the flow Mach number becomes very small. In addition, the ordering of these model terms is similar to their incompressible counterparts. Therefore, the near-wall function ξ can be determined in a manner similar to that proposed in Ref. 27.

The incompressible form of (28) with model terms given in (29) is identical to that proposed in Refs. 26 and 27. In these studies, the coincidence condition suggested by Shima [21] was used to determine ξ. This is equivalent to requiring the modeled ε-equation to achieve balance behavior in the near-wall region at least up to order y. The approach used to deduce ξ is to assumed a functional form for ξ with two undetermined model constants. One of the constant can be determined from near-wall analysis, while the other is evaluated using computer optimization. The ξ function thus determined has been used in Ref. 27 to calculate flat plate boundary-layer flows and in Ref. 26 to calculate fully-developed channel and pipe flows. These calculations were carried out over a wide range of flow Reynolds number. The results were compared with direct simulation data as well as measurements. Very good agreement has been found for both the limiting behavior of the turbulence quantities and ε when compared to direct simulation data [33-35]. Furthermore, the two-equation model calculations of Ref. 27 are found to give better results than those obtained by Speziale et al. [36]. In view of this success, the same approach can be used to determine ξ for compressible flows.

The functional form assumed in Ref. 27 is adopted here, or

$$\xi = f_{w,2}\overline{\rho}\left[-N\frac{\varepsilon\tilde{\varepsilon}}{k} + M\frac{\varepsilon^{*2}}{k}\right], \tag{30}$$

where $f_{w,2}$ is a damping function that goes to one at the wall and zero far away from the wall. It is defined in Ref. 27 as $f_{w,2} = e^{-(Rt/64)^2}$, where $R_t = k^2/\overline{\nu}\varepsilon$ is the turbulent Reynolds number. The function ε^* is defined as $\varepsilon^* = \varepsilon - 2\overline{\nu}k/y^2$ by generalizing the incompressible definition used in Ref. 27. Similarly, $\tilde{\varepsilon}$ is defined with ε_w given by $\varepsilon_w = 2\overline{\nu}(\partial\sqrt{k}/\partial x_j)^2_w$. Once ξ is postulated, the near-wall behavior of (28) and the modeled terms of (29) can be analysed using expansions (21). If the modeled equation is again required to be in balance up to order y, then it can be easily shown that $N = 2 - C_{\varepsilon 2}$ because the mean dilatational terms are of order y. Therefore, to order y^0 they do not contribute to ξ. In Ref. 27, the part involving $C_{\varepsilon 2}$ in N is grouped together with M to give $M_1 = (C_{\varepsilon 2}\varepsilon\tilde{\varepsilon}/\varepsilon^{*2} + M)$ and its value is determined through computer optimization studies. Again, the same procedure is followed in the present study to determine M_1.

Finally, to complete closure of the governing equations, gradient transport is assumed for the Reynolds stresses and the relation is given by

$$-\overline{\rho}\langle u_i'' u_j''\rangle = \overline{\mu}_t\left[\frac{\partial\langle U_i\rangle}{\partial x_j} + \frac{\partial\langle U_j\rangle}{\partial x_i} - \frac{2}{3}\delta_{ij}\frac{\partial\langle U_m\rangle}{\partial x_m}\right] - \frac{2}{3}\delta_{ij}\overline{\rho}k \quad . \tag{31}$$

In addition, a constant turbulent Prandtl number is assumed so that heat and momentum diffusivity can be related by $Pr_t = \overline{\nu}_t/\overline{\alpha}_t$ where $\overline{\alpha}_t$ is the turbulent thermal diffusivity. The damping function f_μ appearing in the definition of $\overline{\mu}_t$ can now be defined. In view of the similarity of the present k and ε equations with those for incompressible flows, the f_μ used in Ref. 27 is adopted here. It is defined as

$$f_\mu = (1 + 3.45/\sqrt{R_t})\tanh(y^+/115) \quad , \tag{32}$$

where $y^+ = yu_\tau/\overline{\nu}$ is the wall coordinate and $u_\tau(x)$ is the friction velocity. In this definition, y is taken to be the normal coordinate and x the stream coordinate.

6. Model Validation

A first step to validate the two-equation model for compressible flows is to apply it to calculate flat plate boundary-layer flows with different wall boundary conditions and free-stream Mach numbers. In this initial attempt, heat flux is not modeled separately. Instead, it is related to momentum flux via the assumption of a constant turbulent Prandtl number. The rationale for doing this is to carefully assess the assumption made in (21) concerning the expansion for ρ', whose validity affects the near-wall analysis used to justify the direct extension of the incompressible near-wall function ξ to compressible flows. By choosing the simplest type of compressible flows to validate the model, a careful analysis of the validity and extent of the expansion for ρ' can be carried out. A second objective of this validation is to determine, if possible, the validity and extent of Morkovin's hypothesis. In other words, it is hoped to evaluate the Mach number range and the type of wall thermal boundary conditions in which the effects of fluctuating density can be neglected in the modeling of the governing equations. Therefore, the experimental data chosen for comparisons are selected from three different groups; one with adiabatic wall boundary condition and varying free-stream Mach number, another with constant wall temperature and varying free-stream Mach number, and finally the variations of skin friction with free-stream Mach number and wall temperature as prescribed by the van Driest II formulae given in Ref. 9. The data for the first two groups are selected from Ref. 31. Only one case with constant wall temperature is selected. The reasons being that the other cases reported in Ref. 31 are either not accurate as far as the measured skin friction is concerned or the measured mean velocity and temperature are doubtful. In the following, the governing equations for compressible flat plate boundary-layer flows are first presented. Then the calculations and comparisons with data are examined and the validity of the two-equation model is studied in detail. Finally, the model performance and its proposed improvement are discussed.

6.1 Governing Equations

Two-dimensional, steady compressible boundary layers on a flat plate are considered. If the usual boundary-layer approximations are made, then equations (9) - (11), (20) and (28) can be substantially simplified. For the sake of completeness, the boundary-layer equations in Cartesian x-y coordinates are listed here as:

$$\frac{\partial}{\partial x}\left(\overline{\rho}\langle U\rangle\right) + \frac{\partial}{\partial y}\left(\overline{\rho}\langle V\rangle\right) = 0 \quad , \tag{33}$$

$$\overline{\rho}\langle U\rangle\frac{\partial\langle U\rangle}{\partial x} + \overline{\rho}\langle V\rangle\frac{\partial\langle U\rangle}{\partial y} = \frac{\partial}{\partial y}\left[(\overline{\mu} + \overline{\mu}_t)\frac{\partial\langle U\rangle}{\partial y}\right] \quad , \tag{34}$$

$$\begin{aligned}\overline{\rho}\langle U\rangle\frac{\partial\langle H\rangle}{\partial x} + \overline{\rho}\langle V\rangle\frac{\partial\langle H\rangle}{\partial y} &= \frac{\partial}{\partial y}\left[\left(\frac{\overline{\mu}}{Pr} + \frac{\overline{\mu}_t}{Pr_t}\right)\right.\\ &\frac{\partial\langle H\rangle}{\partial y} + \overline{\mu}\left(1 - \frac{1}{Pr}\right)\left(1 + \frac{Pr(1 - Pr_t)}{Pr_t(1 - Pr)}\frac{\overline{\mu}_t}{\overline{\mu}}\right)\\ &\left.\langle U\rangle\frac{\partial\langle U\rangle}{\partial y} - \left(\frac{\overline{\mu}}{Pr} + \frac{\overline{\mu}_t}{Pr_t}\right)\frac{\partial k}{\partial y}\right] \quad ,\end{aligned} \tag{35}$$

$$\bar{\rho}\langle U\rangle\frac{\partial k}{\partial x}+\bar{\rho}\langle V\rangle\frac{\partial k}{\partial y}=\frac{\partial}{\partial y}\left[\left(\bar{\mu}+\frac{\bar{\mu}_t}{\sigma_k}\right)\frac{\partial k}{\partial y}\right]+$$

$$\bar{\mu}_t\left(\frac{\partial\langle U\rangle}{\partial y}\right)^2-\frac{2}{3}\bar{\mu}_t\left(\frac{\partial\langle U\rangle}{\partial x}+\frac{\partial\langle V\rangle}{\partial y}\right)^2-\frac{2}{3}\bar{\rho}k\left(\frac{\partial\langle U\rangle}{\partial x}+\frac{\partial\langle V\rangle}{\partial y}\right) \quad (36)$$

$$-\bar{\rho}(\varepsilon+\varepsilon^c),-\gamma\bar{\rho}k\left(\frac{\partial\langle U\rangle}{\partial x}+\frac{\partial\langle V\rangle}{\partial y}\right)+\overline{u''}\frac{\partial}{\partial y}\left(\bar{\mu}\frac{\partial\langle U\rangle}{\partial y}\right)$$

$$\bar{\rho}\langle U\rangle\frac{\partial\varepsilon}{\partial x}+\bar{\rho}\langle V\rangle\frac{\partial\varepsilon}{\partial y}=\frac{\partial}{\partial y}\left[\left(\bar{\mu}+\frac{\bar{\mu}_t}{\sigma_\varepsilon}\right)\frac{\partial\varepsilon}{\partial y}\right]+C_{\varepsilon1}\frac{\varepsilon}{k}\bar{\mu}_t \quad (37)$$

$$\left(\frac{\partial\langle U\rangle}{\partial y}\right)^2-C_{\varepsilon2}\bar{\rho}\frac{\bar{\varepsilon}\bar{\varepsilon}}{k}-\frac{4}{3}\bar{\rho}\varepsilon\left(\frac{\partial\langle U\rangle}{\partial x}+\frac{\partial\langle V\rangle}{\partial y}\right)+\xi\ .$$

In writing down these equations, (33) has been used to relate the shear stress to the mean velocity gradient. It is also noted that G_{ij} is zero for flat plate boundary-layer flows while the only term of importance in T_{ij} is that given by u". If (25) is used to evaluate u", then T_{ij} is of order y^2 and is not important in the near-wall region, which according to So et al. [27] is bounded by $0 \le y^+ \le 5$. The model constants are taken from Refs. 27 and 32 and are given by: $C_\mu = 0.096$, $C_{\varepsilon1} = 1.5$, $C_{\varepsilon2} = 1.83$, $\sigma_k = 0.75$, $\sigma_\varepsilon = 1.45$, $\alpha_1 = 0.15$, $\sigma_\rho = 0.5$ and $\gamma = 0.182$. The turbulent Prandtl number Pr_t is specified as 0.9, while Pr is assumed constant and taken to be 0.74. Sutherland and power laws are used to evaluate fluid viscosity at an appropriate reference temperature. The constants σ_ρ and α_1 are determined by calibrating the calculated results against some classic experiments such as those provided in Refs. 29 and 30. Once determined, they are kept constant for all other calculations. In fact, the cases to be compared in the next section are different from the cases used to calibrate σ_ρ and α_1. As for N and M_1, the final choice of values adopted are 2 and 1.5, respectively, just as in Ref. 27.

The boundary conditions are no slip at the wall for mean velocities and k, and zero heat flux or constant wall temperature at the wall for enthalpy. As for ε, its value at the wall is given by $2\bar{\nu}(\partial\sqrt{k}/\partial y)^2_w$. At the edge of the boundary layer, free-stream conditions are specified for both mean stream velocity and enthalpy. In principle, k and ε should be zero in the free stream. However, in practice, they are assumed to take on some very small values, of the order of 10^{-7}, in the free stream. Thus formulated, the above equations and the appropriate boundary conditions can be solved numerically using the boundary-layer code developed by Anderson and Lewis [30] and modified by So et al. [27].

All measurements used to validate the near-wall two-equation model are drawn from Ref. 31. The calculations are carried out over the range, $0 < M_\infty < 10$, for adiabatic wall boundary condition and over the range, $0 < \Theta_w/\Theta_r < 1$, for constant wall temperature condition. Here, Θ_w is the wall temperature and Θ_r is the recovery temperature for adiabatic wall boundary condition and is the adiabatic wall temperature for constant wall temperature. It should be pointed out that $\Theta_w/\Theta_r = 1.0$ corresponds to adiabatic wall boundary condition while $\Theta_w/\Theta_r < 1$ indicates that the wall is cooled. Since only mean flow properties are available from Ref. 31, comparisons are made with these measurements and another set of calculations using the k-ω model of Wilcox [8]. All comparisons are made at the same momentum thickness Reynolds number (R_θ) as the measurements. Four sets of data are chosen and these are cases 55010504, 53011302 and 73050504 with adiabatic wall boundary condition and case 59020105 with constant wall temperature. The free-stream Mach number (M_∞) for these cases are 2.244, 4.544, 10.31 and 5.29, respectively, while the corresponding R_θ's are 20,797, 5,532, 15,074 and 3,939. Therefore, the data cover a wide range of R_θ and M_∞. The variations of skin friction with M_∞ and Θ_w/Θ_r are compared with the van Driest II formulae reported for a fixed R_θ as specified in Ref. 9. Finally, an assessment of compressibility effects on near-wall flows is attempted by comparing the calculated turbulence statistics for the different cases investigated.

6.2 Comparisons with Data

The results are organized in the following manner for presentation. Mean stream velocities are normalized by u_τ to give u^+ and they are plotted versus ln y^+_w (Fig. 1), where y^+_w is defined as $u_\tau y/\nu_w$. A direct plot of the mean velocities is also given in Fig. 2 where $\langle U\rangle/U_\infty$ versus y/δ is shown. Here, δ is the boundary layer thickness defined as the location of y in which $\langle U\rangle/U_\infty = 1.0$ as specified by the measurements and U_∞ is the free-stream velocity. On the other hand, mean temperatures are normalized by Θ_∞, the free-stream temperature, and are shown versus y/δ (Fig. 3). Plots for the properties, $k^+ = k/u_\tau^2$, $\varepsilon^+ = \varepsilon\bar{\nu}/u_\tau^4$, $-\overline{uv}^+ = -\overline{uv}/u_\tau^2$ and $-\overline{\theta v}^+ = -\overline{\theta v}/U_\infty\Theta_\infty$, are presented in terms of y^+_w and y/δ. Near-wall behavior of k^+, ε^+, $-\overline{uv}^+$ and $-\overline{\theta v}^+$ (Figs. 4 - 7) are discussed first, then the distributions of k^+ and $-\overline{uv}^+$ in the outer region are examined (Figs. 8 and 9). In Figs 8 and 9, δ is not interpreted from measurements; rather it is evaluated at the y location where $\langle U\rangle/U_\infty = 0.9974$. Only the budget of k in the near-wall region for case 73050504 ($M_\infty = 10.31$ and $\Theta_w/\Theta_r = 1.0$) is presented (Fig. 10) because the k budgets for the other cases are essentially similar to that shown in Fig. 10. The effects of Mach number on the asymptotic behavior of k are examined by plotting a_k versus M_∞ (Fig. 11), where a_k is the leading coefficient in the expansion of k^+ in terms of y^+_w. According to Ref. 27, $\varepsilon^+_w = 2a_k$. Therefore, by examining a_k versus M_∞, the variation of ε^+_w with Mach number is also evident. Other asymptotic properties are tabulated in Table 1 for comparison. The variations of skin friction coefficient, $C_f = 2\tau_w/\bar{\rho}_\infty U^2_\infty$, with M_∞ and Θ_w/Θ_r are compared with van Driest II results [9] in Fig. 12. Finally, the mean velocity plots in terms of the compressible u^+ defined as $u^+_c = \left(\int(\bar{\rho}/\bar{\rho}_w)d\langle U\rangle\right)/u_\tau$ for two different M_∞ are shown in Fig. 13. This figure is provided to illustrate the deviation or lack thereof from the van Driest law of the wall for compressible flows [37, 38].

Two versions of the present k-ε model are used to calculate boundary-layer flows. One designated k-ε model/1 solves the k and ε transport equations as given in (38) and (39). The second designated k-ε model/2 solves (38) and (39) with all additional compressible terms neglected and the $\partial k/\partial y$ term omitted in (37). In other words, the two-equation model for k-ε model/2 is a direct variable density extension of the two-equation incompressible model of Ref. 27. These calculations can be used to evaluate the validity and extent of Morkovin's hypothesis and the importance of having an asymptotically consistent near-wall correction for two-equation models.

Four sets of u^+ results are shown in Fig. 1. In the figure, the calculated and measured C_f and the C_f determined from the van Driest II formula of Ref. 9 are listed for comparison. The log-law shown is used to demonstrate the existence of a log region in the calculated and measured flows, while the von Karman constant κ is taken to be 0.41. It is recognized that the intercept is a function of Mach number; however, in this figure, the intercept is taken to be 4.7. The actual value used is not important because the purpose here is to illustrate the slope of the log-law. It can be seen that a log region indeed exists for all calculated and measured flows. The slope is fairly constant for the three adiabatic wall cases tested and the κ thus determined is approximately 0.41. For the cooled wall case, the k-ε model predicted slopes are slightly different from that calculated by k-ω model. None of these slopes yields a von Karman constant of 0.41 though. C_f is predicted correctly by all three models with a

maximum error of less than 5%. For the cooled wall case, the measured C_f is substantially higher than the van Driest II value and, according to Ref. 31, is not as accurate as the measured C_f for the other cases studied. The model calculations are in good agreement with the van Driest II values for all cases examined.

Calculated u^+ profiles correlate well with measurements. At high Mach numbers, there seems to be substantial difference between model predictions and measurements in the outer region of the boundary layer. Such a difference is also noted when the plots are given in terms of $<U>/U_\infty$ versus y/δ in Fig. 2. From these plots, it can be seen that k-ε model predictions of $<U>/U_\infty$ are in better agreement with data than k-ω calculations (Fig. 2). The agreement between k-ε model predictions and measurements is good up to $M_\infty = 10.31$. On the other hand, the discrepancy between calculations and measurements deteriorates as M_∞ increases for the k-ω model. Therefore, the proposed k-ε models represent improvements over existing models whose predictions are correct only for $M_\infty \leq 5$ (see e.g. Ref. 39). Since most existing models do not have an asymptotically consistent near-wall correction and are direct extensions of their incompressible counterparts, the discrepancies display by these models for $M_\infty > 5$ are understandable. Present results show that, if the near-wall flow is modeled in an asymptotically correct and consistent manner, the incompressible models can be straight-forwardly extended to compressible flows with a free-stream Mach number as high as 10. It should be pointed out that the k-ω model is not an asymptotically consistent near-wall model. Therefore, its prediction of $<U>/U_\infty$, in paticular that for the cooled wall case, is not as good as k-ε model calculations. One reason could be the fairly low R_θ (3,939) for this case. Since the results of k-ε model/2 are also in good agreement with measurements (Figs. 1 and 2), the comparisons suggest that the additional compressible terms in (38) and (39) are not too important. However, an examination of the mean temperature results tends not to support this conclusion (Fig. 3).

The mean temperature profile comparisons are shown in Fig. 3. Predictions by the k-ω model show substantial discrepancies compared to the k-ε model calculations and measurements; particularly for the cooled wall case (Fig. 2a). Discrepancies between measurements and k-ω predictions increase as M_∞ increases and as Θ_w/Θ_r decreases. On the other hand, the agreement between k-ε model/1 predictions and data improves as M_∞ increases for adiabatic wall boundary condition. This is not true for k-ε model/2 where the disagreement with data is quite substantial at $M_\infty = 10.31$ (Fig. 2b). The predictions of the cooled wall case (Fig. 2a) tell a different story. It seems that k-ε model/2 gives as good a prediction of the cooled wall case as that of k-ε model/1 (Figs. 1a and 2a). The following three reasons could be put forward to explain this behavior. Firstly, the ρ' expansion may not be totally valid for constant wall temperature boundary condition. Secondly, the proposed compressible models may be more applicable for adiabatic wall boundary condition. Thirdly, the assumption of a constant turbulent Prandtl number may not be appropriate.

The near-wall distributions of k^+ for the four cases are shown in Fig. 4. Only the predictions of k-ε model/1 and k-ω model are compared. The calculations of k-ε model/2 are not shown; instead, the limiting behavior of k^+, $-\overline{uv}^+$ and $-\overline{\theta v}^+$ is tabulated in Table 1 for comparison. In general, the predictions of k-ω model are substantially lowered than those of k-ε model/1. The peaks are about 40% lower than those predicted by k-ε model/1 and the locations where the peaks occur are calculated to be further away from the wall than k-ε model/1 predictions. According to k-ε model/1, the peak of k^+ decreases as M_∞ increases. The decrease is more than 20% over a Mach number range of 10. On the other hand, a slight cooling of the wall at $M_\infty = 5.29$ causes the peak of k^+ to decrease to the same level as that for the case of adiabatic wall with $M_\infty = 10.31$. These results suggest that wall cooling has more influence on reducing turbulent mixing compared to compressibility effects. Overall, compressibility reduces turbulent mixing and the reduction increases with M_∞. The near-wall distributions of ε^+ as calculated by k-ε model/1 are plotted in Fig. 5. It can be seen that the distributions are very similar to those shown in Ref. 27 for incompressible flows. The variations of ε_w^+ with M_∞ and Θ_w/Θ_r are very similar to those of k^+. Again, maximum ε^+ occurs at the wall and a plateau in ε^+ is found in the range, $7 \leq y_w^+ \leq 13$. This means that compressibility has little or no effects on the near-wall behavior of ε^+. The exception is that increases in compressibility and wall cooling tend to decrease ε_w^+.

In general, k-ω model gives a very accurate prediction of $-\overline{uv}^+$ near a wall. Its predictions are as good as those given by k-ε model/1 (Fig. 6). From this set of predictions, the following observations can be made. Firstly, the peak of $-\overline{uv}^+$ decreases with increasing M_∞ and decreasing Θ_w/Θ_r. Secondly, as M_∞ increases and Θ_w/Θ_r decreases, the location of the peak moves towards the wall. Thirdly, the rate of decrease of $-\overline{uv}^+$ in the range, $30 \leq y_w^+ \leq 100$, increases as M_∞ increases. Finally, the asymptotic near-wall behavior of $-\overline{uv}^+$ is listed in Table 1 for comparison. Much the same behavior is also true for $-\theta v^+$ whose distributions in the near-wall region are shown in Fig. 7. If the distributions of $\overline{\theta v}^+$ are plotted instead of $-\overline{\theta v}^+$, the curves will have the same shape as those shown for $-\overline{uv}^+$. Therefore, the observations drawn for $-\overline{uv}^+$ are also valid for θv^+.

The distributions of k^+ and $-\overline{uv}^+$ across the boundary layer are compared in Figs. 8 and 9, respectively. In all cases shown, k-ω model over-predicts k^+ and $-\overline{uv}^+$ in the outer part of the boundary layer compared to the calculations of k-ε model/1. The over-prediction extends across the range, $0.2 \leq y/\delta \leq 1.0$. Reduction of turbulence activities in the outer part of the boundary layer is clearly evident when either compressibility or wall cooling effects are present. The reduction increases as M_∞ increases and Θ_w/Θ_r decreases. Therefore, it is expected that turbulence activities will be substantially reduced in a flow where the free-stream Mach number is large and the wall is highly cooled.

The near-wall k budget for case 73050504 is plotted in Fig. 10. Other budget plots are not shown because they are essentially similar to that given in Fig. 10. It can be seen that the k budget bears a lot of similarity with that calculated for incompressible flows (see e.g. Ref. 27). The additional compressible terms have negligible effect on the near-wall k budget. Therefore, the assumptions made to derive the near-wall function ξ in the dissipation-rate equation are justified. Again, viscous diffusion balances dissipation at the wall. This balance extends to about $y_w^+ = 4$ where turbulent diffusion and production become important. In the region, $4 \leq y_w^+ \leq 15$, viscous and turbulent diffusion, production and dissipation are equally important. Beyond $y_w^+ = 15$, production and dissipation are in balance, just as in the case of incompressible flows. Consequently, the near-wall k behavior is very similar for both incompressible and compressible flows.

According to Refs. 25 and 27, Taylor series expansions about $y_w^+ = 0$ can be assumed for k^+, $-\overline{uv}^+$ and $-\theta v^+$. For incompressible flows, the expansions are valid up to about $y_w^+ = 7$. This range may not be applicable for compressible flows. Nevertheless, such expansions for small y_w^+ can still be assumed. With the help of (21) these expansions can be written as:

$$k^+ = a_k(y_w^+)^2 + b_k(y_w^+)^3 + \ldots\ldots\ldots, \tag{40a}$$

$$-\overline{uv}^+ = a_{uv}(y_w^+)^3 + b_{uv}(y_w^+)^4 + \ldots\ldots, \tag{40b}$$

$$-\overline{\theta v}^+ = a_{v\theta}(y_w^+)^3 + b_{v\theta}(y_w^+)^4 + \ldots\ldots, \tag{40c}$$

where the a's and b's are time-average coefficients that are functions of x. A similar expansion can be deduced for ε^+. Again, using (21), the definition of ε and its wall boundary condition, the expansion for ε^+ can be written as:

$$\varepsilon^+ = 2a_k + 4b_k y_w^+ + \ldots\ldots \qquad (41)$$

From these expansions, it can be easily deduced that $k^{+2}/\varepsilon^+(y_w^+)^2 = 0.5$. Therefore, the asymptotic behavior of $k^{+2}/\varepsilon^+(y_w^+)^2$ is 0.5 and is independent of M_∞ and wall thermal boundary conditions. The accuracy in which a model can predict this quantity is a reflection of the asymptotic consistency of the model. Table 1 shows that k-ε model/1 is indeed asymptotically consistent while k-ε model/2 is not as good. As for the k-ω model, its prediction of this limiting value is poor, therefore, it is not listed in Table 1.

The "a" coefficients can be determined from the calculations and their values are also listed in Table 1 for comparison. It can be seen that a_k varies with free-stream Mach number. A plot of a_k versus M_∞ for adiabatic wall boundary condition is shown in Fig. 11. The value of a_k for the incompressible case is taken from Ref. 27 and is plotted at M_∞ = 0. Clearly, the trend is to approach an asymptotic value for a_k at high M_∞. This decrease in a_k is one of the reason why k decreases for high Mach number flows (Figs 4 and 8). The physical reason is that compressibility tends to hinder turbulence mixing. As a result, both turbulent shear stress and kinetic energy decrease significantly as M_∞ increases (Figs. 4, 6, 8 and 9). Since $\varepsilon_w^+ = 2a_k$ according to (41), dissipation at the wall is also dependent on M_∞. There is no clear trend for a_{uv} and $a_{v\theta}$. However, the values of a_{uv} are consistent with those calculated for incompressible flows [27] and direct simulation data [35]. The value of $a_{v\theta}$ is essentially zero. Since there is no data available, its correctness cannot be verified.

Finally, the ability of the k-ε models to predict skin friction coefficient over a range of M_∞ and wall temperatures is illustrated in Fig. 12. In Fig. 12a, the variation of $C_f/(C_f)_i$ with M_∞ for the case of adiabatic wall boundary condition is shown. Here, $(C_f)_i$ is the skin friction coefficient for an incompressible flow evaluated at $R_\theta = 10^4$ and is determined to be 2.73×10^{-3}. The figure shows a comparison of the calculations of k-ε model/1 and k-ε model/2 with the van Driest II distribution. Below M_∞ = 5, the calculated variations of $C_f/(C_f)_i$ with M_∞ are slightly lower than the van Driest II distribution but they are slightly higher beyond M_∞ = 5. Essentially, there is no difference between the predictions of k-ε model/1 and k-ε model/2. This means that both versions of the k-ε model give a correct prediction of the $C_f/(C_f)_i$ variation with M_∞ for adiabatic wall boundary condition. The predictions for the cooled wall case are not as good, especially at low temperature ratio (Fig. 12b). Three sets of calculations are presented. These are k-ε model/1, k-ε model/2 and a third version of k-ε model/1 with the $\partial k/\partial y$ term in (37) neglected. Calculations for this case are carried out at M_∞ = 5, $R_\theta = 10^4$ and the incompressible C_f is again determined to be 2.73×10^{-3}. It can be seen that error of 5% or larger starts to accumulate at approximately $\Theta_w/\Theta_r = 0.4$ for k-ε model/1. This trend is contrary to previous calculations [8]. An examination of the governing equations solved by other researchers revealed that, besides differences noted in the turbulence model equations, the mean energy equation solved by these researchers does not include the term $\partial k/\partial y$ in the right hand side of (37). Indeed, when the $\partial k/\partial y$ term is neglected, an overall improvement is obtained. The predicted C_f at Θ_w/Θ_r = 0.2 is increased by about 6%, thus giving a better agreement with the van Driest II formula. If the additional compressible terms in the k-ε equations are further neglected (k-ε model/2), the calculated C_f is only improved by about 3%. The remaining disagreement could be attributed to the assumption of a constant turbulent Prandtl number. When $Pr_t = 0.7$ is assumed, the calculations are in even better agreement with data. The reason could be due to a further reduction of turbulent mixing as a result of the wall being cooled. However, this effect has not been appropriately accounted for in the models, particularly their near-wall behavior. In other words, if highly cooled-wall flows are to be predicted correctly, heat fluxes should be modeled separately rather than linking to momentum fluxes via a constant turbulent Prandtl number.

6.3 Discussion

In the past, velocity profiles in wall coordinate were invariably plotted in terms of u_c^+ to illustrate the existence of the log-law and the constancy of κ in compressible boundary-layer flows. The proposal was first suggested by van Driest [37] and later confirmed by Maise and McDonald [38] when they analysed ten sets of data in the Mach number range of 0 - 5. Since then, the compressible law of the wall is taken to be given by u_c^+ rather than by u^+ and κ is considered to be about 0.41 and constant over the Mach number range of 0 - 5. The calculated and measured velocity plots given in Fig. 1 show support for the compressible law of the wall when it is written in terms of u^+ rather than u_c^+. Furthermore, κ is determined to be approximately 0.41 and is relatively constant over the Mach number range of 0 - 10. These results seem to conflict with the proposal of van Driest [37]. In order to resolve this seeming contradiction, the velocity plots of u_c^+ versus ln y_w^+ for cases 55010504 (M_∞ = 2.244, Θ_w/Θ_r = 1) and 53011302 (M_∞ = 4.544, Θ_w/Θ_r = 1) are shown in Fig. 13. In addition, the compressible law of the wall as given in Ref. 38 is shown for comparison. It can be seen that a line that is parallel to the compressible law of the wall can be drawn through a few of the data points spanning over a narrow range of y_w^+. On the other hand, the calculated profiles are in agreement with data over a wider range of y_w^+. The slopes of the calculated profiles are roughly parallel and are slightly larger than the slope of the compressible law of the wall shown. Therefore, irrespective of how the velocity profiles are plotted, the calculations are in good agreement with data. However, the slope of the log-law is given by 1/0.41 only when the profiles are plotted in terms of u^+.

7. Conclusions

The k and ε equations for compressible flows are derived by assuming that there is no dynamical similarity between the compressible and incompressible fields. Therefore, the influences of fluctuating density on the mean and turbulence fields have to be accounted for in the modeled equations. This can be accomplished by first re-casting the exact k and ε equations into forms that are similar to their incompressible counterparts. In other words, the viscous diffusion and dissipation functions have to be defined exactly like their incompressible terms. This procedure gives rise to additional terms in the k and ε equations. These terms depend explicitly on compressibility and vanish when the fluid density becomes constant. One extra term in the k-equation is related to fluid dilatation and can be interpreted as compressible dissipation. The others are production terms that depend on the gradients of the mean pressure and mean viscous shears. All additional terms are found to be relatively unimportant in the near-wall region, or $0 \le y_w^+ \le 50$. This realization, therefore, allows the near-wall incompressible models to be extended directly to compressible flows without modifications, while still maintaining the balance of the modeled equations as a wall is approached. Models are proposed for the additional terms in the k and ε equations. The constants introduced by the new models are determined by calibrating the calculations against measurements in compressible flows.

The near-wall two-equation model is used to calculate compressible flat plate boundary-layer flows with different wall thermal boundary conditions and free-stream Mach numbers.

Comparisons are made with various mean flow measurements and with calculations of the k-ω model. Good agreement is obtained between the present calculations and measurements. In particular, the log-law for compressible flows is recovered and the slope of the log-law is found to be fairly independent of free-stream Mach number for the range, $0 \le M_\infty \le 10$, tested. Even though k-ω model gives a correct prediction of u^+ versus ln y_w^+, their velocity comparison in terms of $<U>/U_\infty$ versus y/δ shows substantial discrepancy with data. The discrepancy increases with increasing Mach number and can be attributed to a near-wall behavior that is not asymptotically correct.

The following conclusions can also be drawn from the above analysis. Firstly, Morkovin's hypothesis is valid up to a free-stream Mach number of about 5 for flat plate boundary-layer flows with adiabatic wall boundary condition. This means that the effects of fluctuating density are becoming more and more important as M_∞ increases beyond 5. Secondly, the assumption of a constant turbulent Prandtl number is not appropriate for cooled wall thermal boundary condition. The reason is further reduction in turbulent mixing due to a cooled wall and this effect is not correctly accounted for in a constant turbulent Prandtl number approach. Most likely a heat flux model is required if the characteristics of cooled-wall compressible boundary-layer flows are to be predicted correctly. Thirdly, it is important to model the near-wall flow correctly if the overall boundary-layer characteristics are to be predicted with confidence. This point is substantiated by the k-ε model calculations where all additional compressible terms in the turbulence equations are neglected. These results are in good agreement with measurements even though they differ slightly from the predictions of k-ε model/1 where all the additional terms are retained. In other words, an asymptotically consistent near-wall model is more important to the prediction of compressible boundary-layer flows than the inclusion of fluctuating density effects in the modeled equations. Fourthly, the predicted near-wall characteristics are very similar to those calculated for incompressible flows. In the range of free-stream Mach number tested, the calculated near-wall characteristics are essentially independent of Mach number and wall thermal boundary condition. Very near the wall, viscous diffusion of k is balanced by the dissipation of k. Beyond $y_w^+ = 15$, dissipation is balanced by mean shear production of k. In between these two regions, viscous and turbulent diffusion of k, production of k and dissipation of k are of importance in the budget of k. The additional compressible terms in the k-equation are essentially negligible in the near-wall region up to $y_w^+ = 50$. This is the reason why the model also performs well when the additional compressible terms are neglected in the equations. Finally, the term $\partial k/\partial y$ in the mean energy equation makes a significant contribution to the calculated C_f in the highly cooled wall case. Traditionally, this term is neglected. However, present analyses show that even though it is relatively unimportant in flows with adiabatic wall boundary condition, it cannot be neglected in flows with a highly cooled wall. The inclusion of this term degrades the prediction of C_f. It is believed that the degradation is a result of an incorrect modeling of turbulent heat flux. Therefore, improvements should be directed at the relaxation of the constant turbulent Prandtl number assumption.

Acknowledgement

This work was supported by NASA Langley Research Center, Hampton, Virginia 23665, under Grant No. NAG-1-1080.

References

[1] Wilcox, D.C. and Alber, I.E., "A turbulence model for high speed flows," Proc. of the 1972 Heat Transfer and Fluid Mechanics Institute, Stanford University Press, 1972, pp. 231-252.

[2] Bradshaw, P., "Compressible turbulent shear layers," Annual Review of Fluid Mechanics **9**, 1977, pp. 33-64.

[3] Rubesin, M.W., "A one-equation model of turbulence for use with the compressible Navier-Stokes equations," NASA TM-X-73-128, 1976.

[4] Viegas, J.R., and Horstman, C.C., "Comparison of multiequation on turbulence models for several shock boundary layer interaction flows," AIAA Journal **17**, 1979, pp. 811-820.

[5] Vandromme, D., Ha Minh, H., Viegas, J.R., Rubesin, M.W. and Kollman, W., "Second order closure for the calculation of compressible wall bounded flows with an implicit Navier-Stokes solver," 4th Turbulent Shear Flows Conferences, Karlsruhe, 1983, pp. 1.1-1.6c.

[6] Saffman, P. G. and Wilcox, D. C., "Turbulence-Model Predictions for Turbulent Boundary Layers," AIAA Journal, **12**, 1974, pp. 541-546.

[7] Coakley, T. J., "Turbulence modeling methods for the compressible Navier-Stokes equations," AIAA Paper 83-1693, 1983.

[8] Wilcox, D. C., "Reassessment of the scale-determining equation for advanced turbulence models," AIAA Journal, **26**, 1988, pp. 1299-1310.

[9] Kline, S. J., Cantwell, B. J. and Lilley, G. M. (eds.), *Proceedings of the 1980-81 AFOSR-HTTM-Stanford Conference on Complex Turbulent Flows*, Stanford University Press, Stanford, CA, 1981.

[10] Morkovin, M., "Effects of compressibility on turbulent flows," Mecanique de la turbulence, C.N.R.S., edited by A.Favre, 1962, pp. 367-380.

[11] Bradshaw, P., "The effect of mean compression or dilatation on the turbulence structure of supersonic boundary layers," Journal of Fluid Mechanics **63**, 1974, pp. 449-458.

[12] Oh, Y.H., "Analysis of two-dimensional free turbulent mixing," AIAA Paper No. 74594, 1974.

[13] Speziale, C. G. and Sarkar, S., "Second-Order Closure Models for Supersonic Turbulent Flows," AIAA Paper No. 91-0217, 1991.

[14] Rodi, W., "Recent developments in turbulence modeling," Proc. 3rd Int. Symp. on Refined Flow Modelling and Turbulence Measurements, Tokyo, July 26-28, 1988.

[15] Launder, B.E. and Tselepidakis, D.P., "Contribution to the second-moment modeling of sublayer turbulent transport," Proc. Zaric Memorial International Seminar on Wall Turbulence, Dubrovnik, Yugoslavia, 1988.

[16] Speziale, C. G., "Analytical methods for the development of Reynolds-stress closures in turbulence," Annual Review of Fluid Mechanics, **23**, 1991, pp. 107-157.

[17] So, R. M. C., Lai, Y. G., Zhang, H. S. and Hwang, B. C., "Near-wall second-order turbulence closures: a review," AIAA Journal, 1991, to appear.

[18] Cousteix, J., "Three-dimensional and unsteady boundary layer computation," Annual Review of Fluid Mechanics **18**, 1986, pp. 173-196.

[19] Hanjalic, K. and Launder, B.E., "Contribution towards a Reynolds-stress closure for low-Reynolds-number turbulence," Journal of Fluid Mechanics **74**, 1976, pp. 593-610.

[20] So, R.M.C. and Yoo, G.J., "Low-Reynolds-number modeling of turbulent flows with and without wall transpiration," AIAA Journal **25**, 1987, pp. 1556-1564.

[21] Shima, N., "A Reynolds-stress model for near-wall and low-Reynolds-number regions," Journal of Fluids Engineering **110**, 1988, pp. 38-44.

[22] Yoo, G.J. and So, R.M.C., "Variable density effects on axisymmetric sudden-expansion flows," International Journal of Heat and Mass Transfer **32**, 1989, pp. 105-120.

[23] Launder, B.E., "On the computation of convective heat transfer in complex turbulent flows," Journal of Heat Transfer **110**, 1988, pp. 1112-1128.

[24] Nagano, Y. and Kim, C., "A two-equation model for heat transport in wall turbulent shear flow," Journal of Heat Transfer **110**, 1988, pp. 583-589.

[25] Lai, Y.G. and So, R.M.C., "Near-wall modeling of turbulent heat fluxes," International Journal of Heat and Mass Transfer, 33, 1990, pp. 1429-1440.

[26] Lai, Y.G. and So, R.M.C., "On near-wall turbulent flow modeling," Journal of Fluid Mechanics, 221, 1990, pp. 641-673.

[27] So, R.M.C., Zhang, H.S. and Speziale, C.G., "Near-wall modeling of the dissipation-rate equation," AIAA Journal, 1991, to appear.

[28] Sarkar, L, Erlebacker, G., Hussaini, M.Y. and Kreiss, H.O., "The analysis and modeling of dilatational terms in compressible turbulence," NASA CR-181959, 1989.

[29] Coles, D., "Measurements of turbulent friction on a smooth flat plate in supersonic flow," Journal of Aeronautical Sciences **21**, 1954, pp. 433-448.

[30] Anderson, E. C. and Lewis, C. H., "Laminar or turbulent boundary-layer flows of perfect gases or reacting gas mixtures in chemical equilibrium," NASA CR-1893, 1971.

[31] Fernholz, H. H. and Finley, P. J., "A critical compilation of compressible turbulent boundary layer data," AGARDograph No. 223, 1977.

[32] Jones, W.P., "Models for turbulent flows with variable density and combustion," **Prediction Method for Turbulent Flows**, (Edited by W. Kollenann), Hemisphere, London, 1980, pp. 379-422.

[33] Mansour, N.N., Kim, J. and Moin, P., "Reynolds-stress and dissipation-rate budgets in a turbulent channel flow," Journal of Fluid Mechanics, **194**, 1988, pp. 15-44.

[34] Mansour, N.N., Kim, J. and Moin, P., "Near-wall k-ε turbulence modeling," AIAA Journal, **27**, 1989, pp. 1068-1073.

[35] Spalart, P.R., "Direct simulation of a turbulent boundary layer up to R_θ = 1410, " Journal of Fluid Mechanics, **187**, 1988, pp. 61-98.

[36] Speziale, C. G., Abid, R. and Anderson, E. C., "A critical evaluation of two-equation models for near-wall turbulence," AIAA Paper No. 90-1481, 1990.

[37] Driest, E. R. van, "Turbulent Boundary Layer in Compressible Fluids," Journal of Aeronautical Sciences, **18**, 1951, pp.145-160 and 216.

[38] Maise, G. and McDonald, H., "Mixing Length and Kinematic Eddy Viscosity in a Compressible Boundary Layer," AIAA Journal, **6**, 1968, pp. 73-80.

[39] Bradshaw, P., Launder, B. E. and Lumley, J. L., "Collaborative Testing of Turbulence Models," *Journal of Fluids Engineering*, **113**, 1991, pp.3-4.

Case	M_∞	Θ_w/Θ_r	Model	a_k	$a_{uv}x10^4$	$a_{v\theta}x10^7$	$k^+/\varepsilon^+(y_w^+)^2$
55010504	2.244	1.0	k-ε model/1	0.0987	7.167	-0.465	0.50
55010504	2.244	1.0	k-ε model/2	0.0992	7.198	-0.998	0.50
53011302	4.544	1.0	k-ε model/1	0.0824	6.700	-6.44	0.50
53011302	4.544	1.0	k-ε model/2	0.0836	6.760	-11.79	0.50
73050504	10.31	1.0	k-ε model/1	0.0741	6.630	89.5	0.50
73050504	10.31	1.0	k-ε model/2	0.0771	6.740	-131.0	0.51
59020105	5.29	0.92	k-ε model/1	0.0784	6.120	11.1	0.50
59020105	5.29	0.92	k-ε model/2	0.0788	6.140	-5.88	0.50

Table 1. Asymptotic near-wall behavior of the turbulence properties.

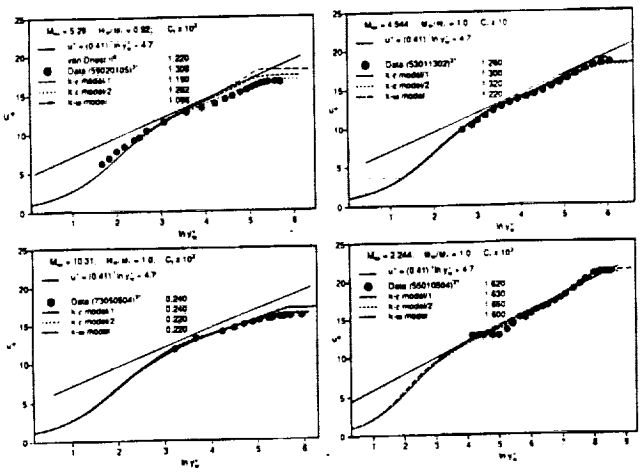

Figure 1. Comparison of calculated u^+ with measurements.

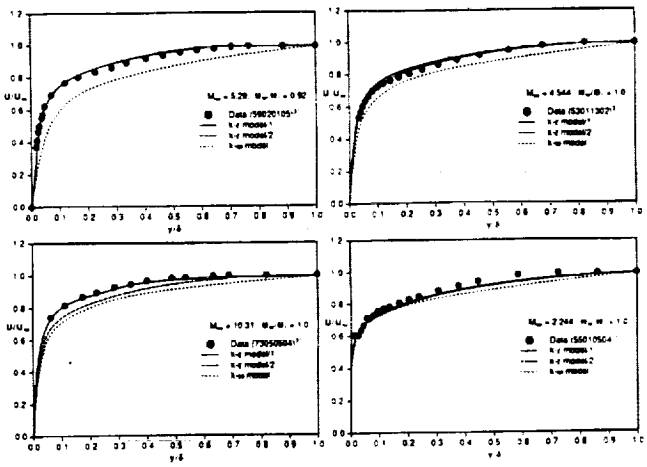

Figure 2. Comparison of calculated $\langle U \rangle / U_\infty$ with measurements.

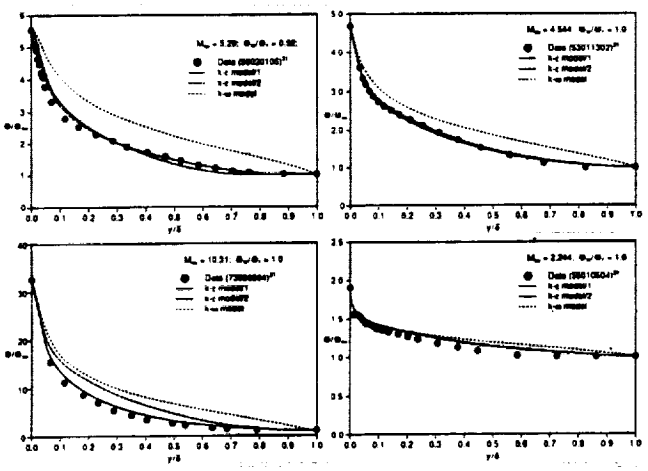

Figure 3. Comparison of calculated mean temperatures with measurements.

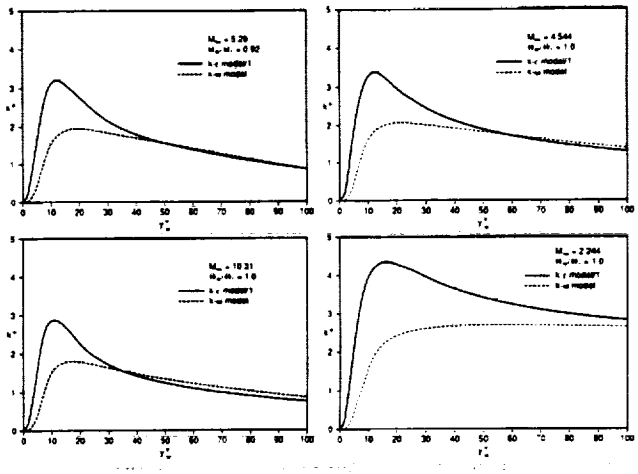

Figure 4. Near-wall distributions of turbulent kinetic energy.

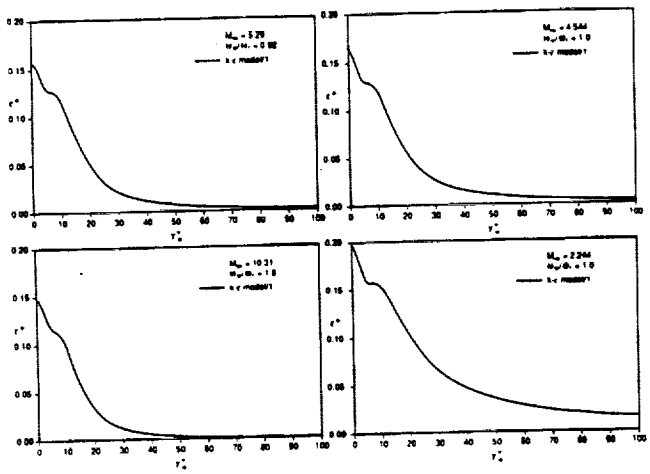

Figure 5. Near-wall distributions of the solenoidal dissipation rate of the turbulent kinetic energy.

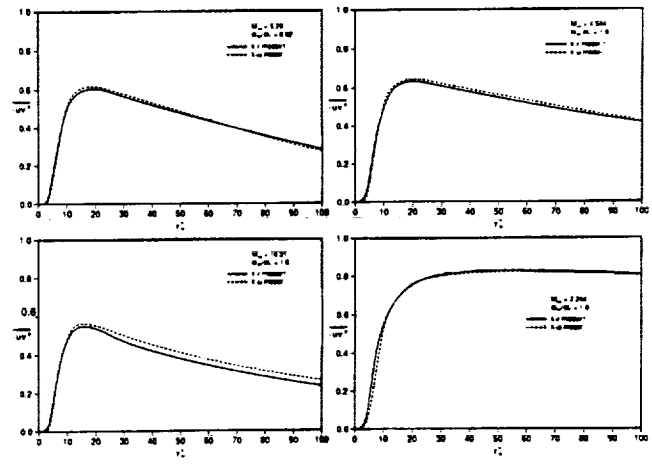

Figure 6. Near-wall distributions of Reynolds shear stress.

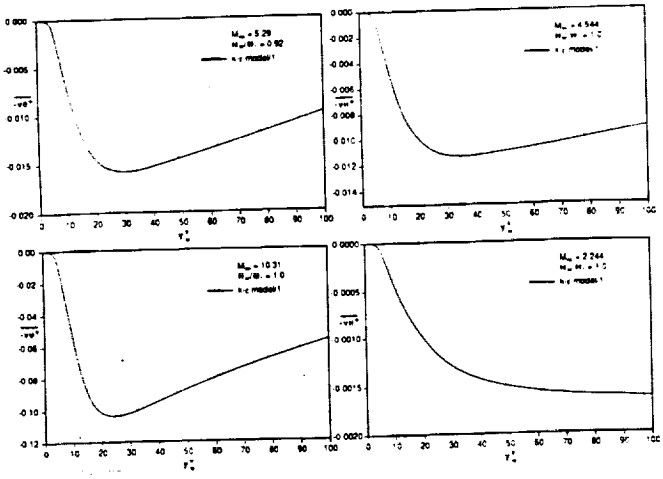

Figure 7. Near-wall distributions of Reynolds heat flux.

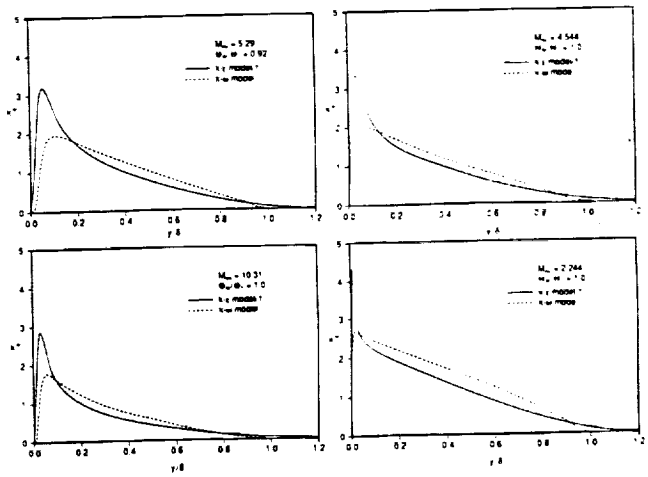

Figure 8. Turbulent kinetic energy distributions across the boundary layer.

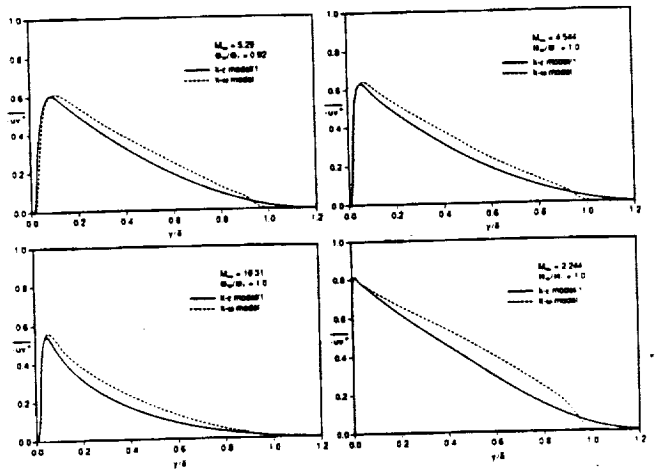

Figure 9. Reynolds shear stress distributions across the boundary layer.

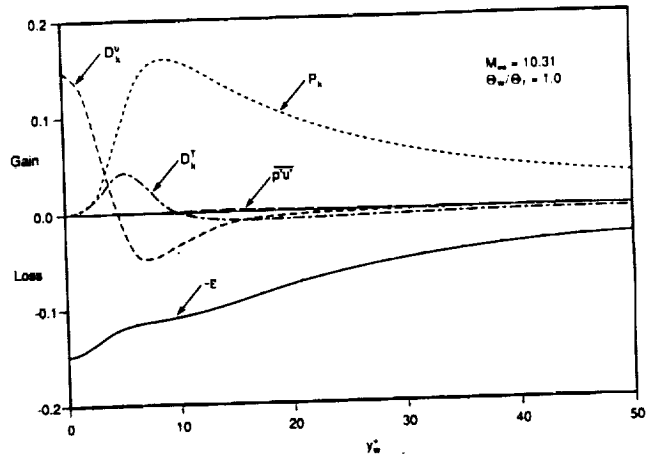

Figure 10. Near-wall k budget for the case with M_∞ = 10.31 and adiabatic wall boundary condition.

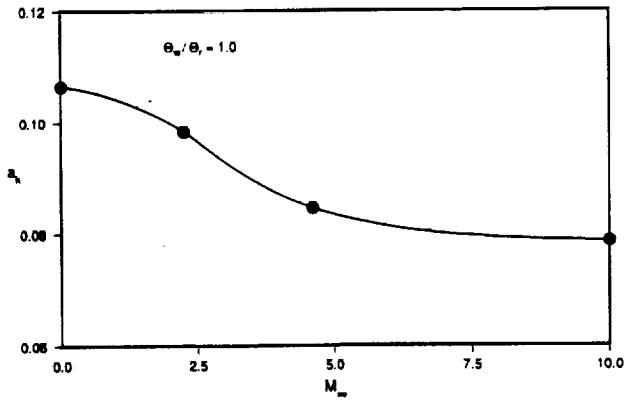

Figure 11. Variation of the slope of k^+ at the wall with M_∞.

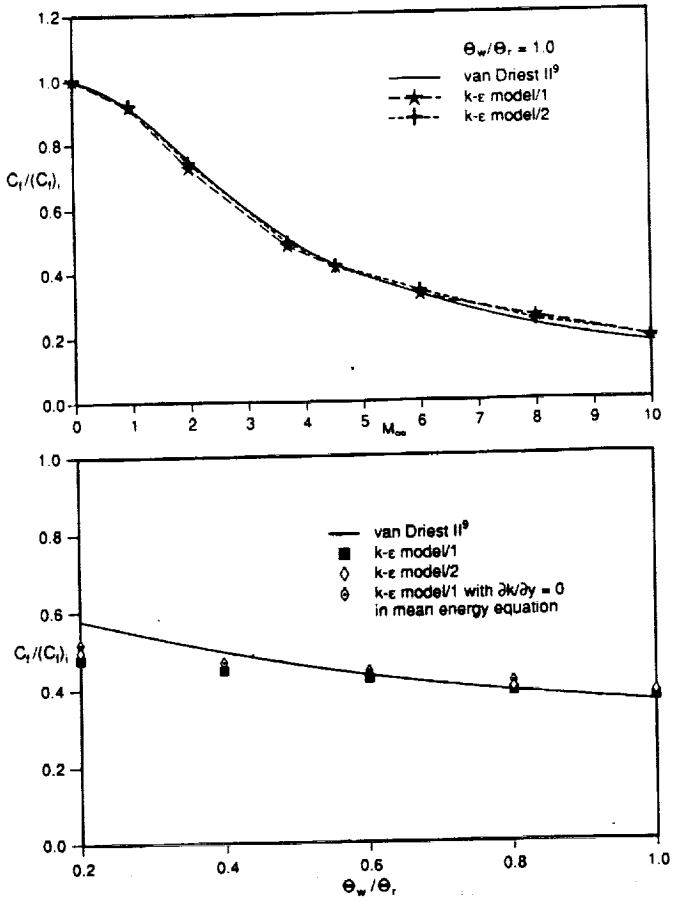

Figure 12. Skin friction coefficient variations with M_∞ and Θ_w/Θ_r.

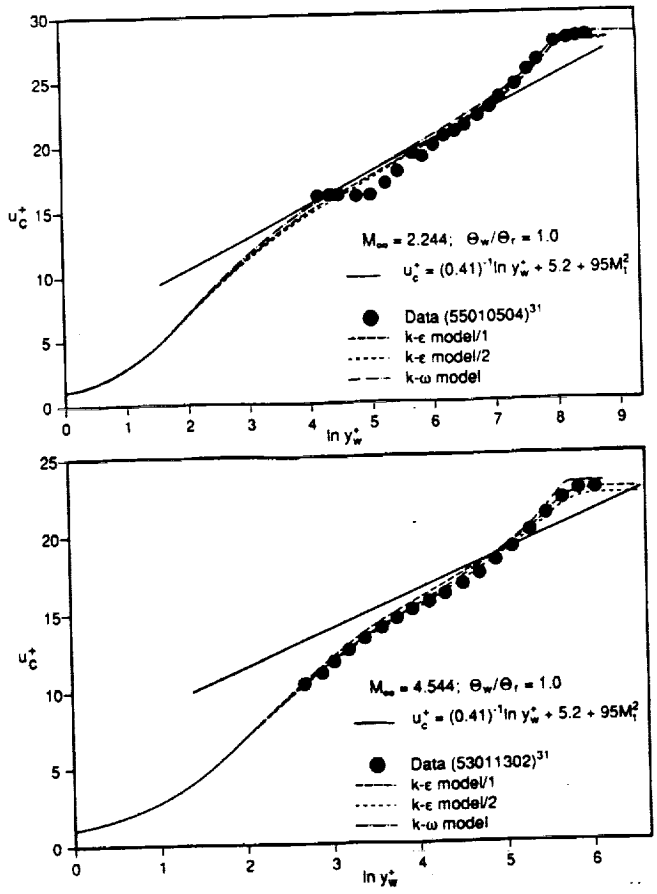

Figure 13 Mean velocity plots in terms of van Driest variable u_c^+ for cases 55010504 and 53011302.